Novel dense skin hollow fiber membrane contactor based process for CO2 removal from raw biogas using water as absorbent

Bouchra Belaissaoui, Eric Favre

Novel dense skin hollow fiber membrane contactor based process for CO_2 absorption from raw biogas and stripping using water as absorbent

Bouchra Belaissaoui, Eric Favre*

LRGP-CNRS Université de Lorraine, 1 rue Grandville 54001 Nancy, France

Manuscript submitted to separation and purification technology

*Corresponding author: Tel: +33 372 74 37 98; fax : +33 383 32 29 75
E-mail address: bouchra.belaissaoui@univ-lorraine.fr (B.Belaissaoui)

Abstract

CO_2 removal produced biogas is required in order to meet standards for the gas grid or as a vehicle fuel. Among biogas upgrading available techniques, pressurized water absorption using packed column (PWA) is one of the most well-established technique. In this work, a novel absorption/desorption loop using dense based Hollow Fiber Membrane Contactor (HFMC) process for CO_2 removal from raw biogas using water as absorbent is proposed and investigated by simulation. Thanks to ability of dense membrane to withstand a high transmembrane pressure, neither water depressurization before the desorber nor water recompression before the absorber is needed. 1D modeling based on a resistance in series approach is used for the modeling of both absorption and desorption units. HFMC based process performances are compared to state of the art packed column based process reported in literature. Using commercially available dense based HFMC, the process is able to recover 96.6 % of CO_2 and reach biomethane purity of 98%. The corresponding energy requirement is of 0.17 kWh/Nm^3 of raw biogas, which is 20 to 35% lower than that reported for packed column based process, under comparable gas inlet conditions and product specifications. However, methane loss in the investigated operating conditions is around 8 % which is higher than that reported for conventional packed column based process where the value is less than 2%. The novel HFMC process offers absorption intensification factor of about 1.68, corresponding to a volumetric reduction of about 68% of the absorption unit. Given that liquid side mass transfer coefficient is about one to two orders of magnitude lower than that of the membrane, process selectivity is mainly controlled by the absorbent selectivity. Under the investigated operating conditions, no significant methane loss reduction is obtained from increasing membrane selectivity from 17 to 60 with membrane mass transfer coefficient of 5.10^{-4} and 5.10^{-5} m/s respectively.

Keywords

Biogas, water absorbent, physical absorbent, hollow fiber membrane contactor, gas-liquid absorption, simulation.

Highlights

- Energy requirement of dense HFMC based process is 20 to 35% lower than that reported in literature for packed column.
- Methane loss under the investigated operating conditions is around 8 % which is higher than values reported for packed column (below 2%).
- The process can offer absorption intensification factor of about 1.68, corresponding to a volumetric reduction of about 68% of the absorber.
- Liquid side mass transfer coefficient is about one and two orders of magnitude lower than of the membrane in absorber and desorber respectively.
- In the investigated conditions, process selectivity is mainly controlled by the selectivity of the absorbent.

1- Introduction

Biogas is produced from anaerobic digestion of organic waste material and is mainly composed of CH_4 (typically 55 - 65 %) and CO_2 (typically 35 - 45 %) with smaller proportions of H_2S, water vapor and other minor compounds (N_2, O_2, H_2S or NH_3). After purification, biomethane can be used as a renewable energy source in combined heat and power plants, as vehicle fuel or as a substitute for natural gas [**Raven and Gregersen, 2005**]. Biogas upgrading involves the removal of carbon dioxide and other impurities (**Figure 1**). Typically, methane concentration over 97% is required (see **Table A1** in **Appendix A).**

Several technologies for biogas upgrading are commercially available and others are at the pilot or demonstration plant level: pressurized water absorption (PWA), Physical absorption (PhyA), chemical absorption (ChemA), pressure swing adsorption (PSA) and membrane separation (MemS). Among more than 200 biomethane plants in European region, PWA is one of the most energy efficient and well-established techniques, used in at almost 40 % of all biomethane plants **[IEA report, 2013, Persson, 2003].** Water effectively combines major advantages for the removal of gas impurities through an absorption process: large availability, low cost and it is a green solvent compared to organic liquids. Moreover, contrary to ChemA, PWA requires a simple process design because absorbent regeneration is achieved using a simple solvent depressurization (no heat exchangers or reboilers are needed).

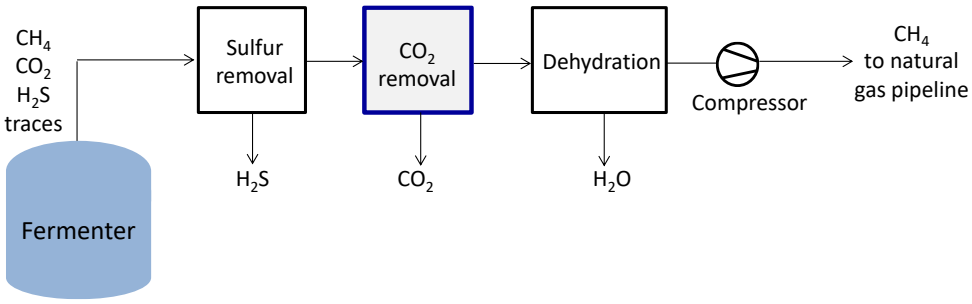

Figure 1: *Illustration of typical biogas upgrading process from the fermenter to the natural gas grid.*

However, upgrading leads to supplementary cost in addition to the costs of biogas production. Thus, an energy efficient upgrading process minimizing equipment and installation size is required.

Hollow fiber Membrane contactors (HFMC) are considered as one of the most promising technology to achieve intensified gas-liquid mass transfer thanks to their very high interfacial area, up to 30 times of that encountered in packed columns (**Figure 2**). The supplementary mass transfer resistance of the membrane is shown to be compensated by the much larger specific interfacial area. In addition, membrane contactors provide independent regulation of gas and liquid flows and are insensitive to module-orientation, which make them very effective in comparison to conventional equipment for offshore application. A comprehensive general review on membrane contactors can be found in **Gabelman and Hwang**, 1999 and **Drioli *et al.*, 2005**.

Carbon dioxide absorption in water using HFMC has been investigated by several authors. A brief literature summary can be found in our previous article [**Belaissaoui *et al.*, 2016**]. However, these studies are almost systematically based on porous hydrophobic membranes where pore wetting has been reported to occur, reducing significantly the separation performance and limiting the operating conditions. Moreover, in physical absorption, liquid mass transfer resistance is predominant with mass transfer coefficient about two orders of magnitude lower compared to chemical absorption coefficient, thus either composite or self-standing dense materials can be used.

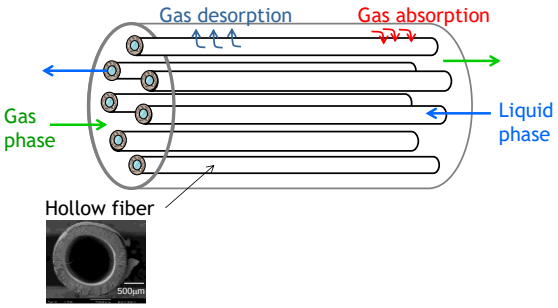

***Figure 2**: Illustration of hollow fiber membrane contactor for gas absorption and desorption using liquid absorbent*

Dense membrane material has been shown to be particularly attractive:

(i) The mechanical resistance offered by dense material membranes opens up unique possibilities for increased energy efficiency as the liquid solvent can be maintained under pressure during the regeneration step.

(ii) Thanks to their ability to prevent membrane wetting phenomena because no pores are present, liquid pressure can be set independently of gas pressure.

(iii) Dense membrane contactors offer a unique opportunity for methane losses limitation, based on the possibility of commercial membrane modules to offer CO_2/CH_4 membrane selectivity from 10 to above 60 [**Belaissaoui *et al.,* 2016**].

The potentiality of either composite or self-standing dense materials remains however largely unexplored for pressurized water absorption in biogas purification at the exception of few studies [**Ozturk and Hughes (2012), Trusov *et al*., 2011, Heile et al., (2014), Belaissaoui et al., (2016) , Kerber et al., 2016**]. Moreover, in all these studies, no values have been given of intensification factor as well as methane loss under industrial relevant conditions for both absorption and desorption steps, with the specification of methane purity (> 98%). Additionally, to our knowledge, the evaluation of the corresponding energy requirement of HFMC for this application, using the potentialities exposed above and offered by dense membrane contactor has not been addressed.

In the present paper, a novel absorption/ desorption loop using dense based Hollow Fiber Membrane Contactor (HFMC) technology for biogas purification by pressurized water is proposed and investigated by simulation. 1D modeling based on a resistance in series approach is used for the modeling of both absorption and desorption units. HFMC based process performances are compared to those of state of the art packed column based process reported in literature. The intensification potential of dense skin membrane contactors compared to packed column, methane loss and specific energy requirement are evaluated and discussed.

2. Conventional packed column for CO_2 removal from biogas using HPWS

In this study, we have considered the state of the art packed column based HPWS as a reference. The standard HPWS process, shown in **Figure 3**, makes use of two packed columns (absorption and regeneration unit) with a pressurized water recycling loop. Given that raw biogas is available at near atmospheric pressure, it needs to be compressed up to 6-10 bar in order to increase the driving force of the separation. The raw biogas is normally cleaned before compression to remove water and hydrogen sulfide. In cases where ammonia, siloxanes and volatile organic carbons are expected in significant concentrations, these components are also commonly removed before the biogas upgrading. Water is removed to prevent condensation during compression. Compression raises biogas temperature and would decrease CO_2 solubility, thus, a gas cooling is required prior to the absorber. Because CO_2 loaded solvent in generated by depressurization up to atmospheric pressure; solvent recompression up to absorber pressure is needed, leading to subsequent energy pumping demand.

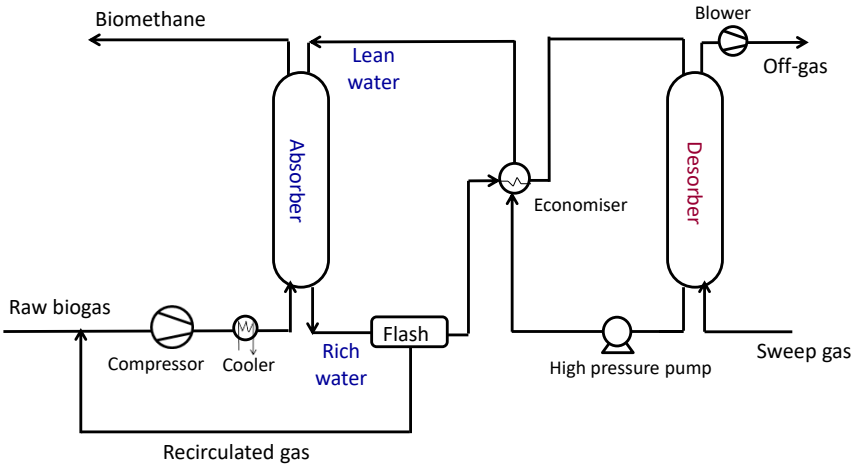

***Figure 3**: Simplified process flow diagram of state of the art pressurized water absorption (PWA) process*

In order to limit methane loss, water leaving the absorption column is transferred to a flash tank at pressure about 2 bar and the released gas is recycled to the biogas inlet**.** It is reported that PWA process has a slip of about 1% in modern plants [**Bauer et al., 2013**]. It was reported that without a flash tank CH_4 losses of 6% are encountered when operating at pressure of 10 bar [**Nock et al., 2014]**. By reducing the pressure below 5 bar, CH_4 loss drops to around 3%. Compared to other techniques, ChemA system using amine absorbent has a much lower CH_4 slip with 0.1% guaranteed. In order to further minimize the loss of methane and its release to the atmosphere, the treatment of the off-gas, air or water streams leaving the plant is needed. One way of limiting the methane slip is to mix the off-gas with air that is used for combustion. Alternatively, methane can be oxidized by thermal or catalytic oxidation. **Table 1** provides a comparison of different technology performances in term of energy requirement, methane loss and methane purity.

***Table 1**: Comparison of the specific energy requirement of different technologies for biogas purification. Data from literature.*

	Pressurized water absorption (PWA)	Chemical absorption using Amine (ChemA)	Pressure swing adsorption (PSA)	Membrane separation (MemS)	Physical absorption (PhyA)
Electric energy demand in kWh/Nm^3 raw biogas	0.23-0.3 [a] 0.2-0.3 [b] <0.25 [c]	0.12-0.15 [a] 0.05-0.14 [b]	0.25-0.3 [b] 0.2-0.3 [a]	0.2-0.28 [b] 0.2-0.3 [a]	0.23-0.29[a]
Thermal energy demand in kWh/Nm^3 raw biogas	-	~ 0.55 [b] at 100-150°C	-	-	-
Product pressure in bar	6-10[a] 4-7[d]	1.1[d]	4-7[d]	5-9 [b]	-
CH_4 loss (%)	1-2 [b] 1 [a] <1-2 [c]	<0.01[b] <0.1[a]	1-5[b] 1.8-2 [a]	0.5-10 [b] ~0.5 [a]	2[e] 0.5-2 [f]
CH_4 purity (%)	>97[a]	96-97[a] 99.8 [a]	97[a]	>98[a] 98 [b]	98[a]
[a] Bauer, et al., 2013, [b] Garnaud and Zick, 2014, [c] Petersson and wellinger, 2009, [d] Scholz et al., 2013 e Persson (2003), [f] Hoyer et al., 2016					

The power requirement of water scrubbing varies depending on plant configuration and pressure used.

Generally, there is a lack of published work investigating the energy requirements of CO_2 water scrubbing process [**Budzianowski 2017]**. Providers of commercial water absorption installations indicate basic characteristic and few technical details are revealed. Literature values show some disagreement, with many of the reported values given in different units and under different operational conditions [**Nock 2014**]. The energy requirement of PWA is generally in the range 0.2-0.3 kWh per Nm^3 of raw biogas depending on the pressure, configuration used and methane specification **[Bauer et al., 2013].**

3. Novel HFMC based absorption/desorption loop for biogas purification by pressurized water

An illustration of absorption and desorption using dense skin based membrane contactors is presented in **Figure 4. Figure 5** shows the novel HFMC based absorption/desorption loop for biogas purification by pressurized water. First, biogas is compressed and cooled before entering the absorber. CO_2 enriched water with some dissolved methane, leaving the absorber is sent to the desorber, without depressurization. Indeed, as explained above, dense membrane is able to withstand high transmembrane pressure difference. CO_2 rich solvent meets then a counter flow of air sweep in the desorber, where carbon dioxide is released with a certain amount of lost methane. The regenerated water leaving the desorber is recycled back to the absorber in a closed loop.

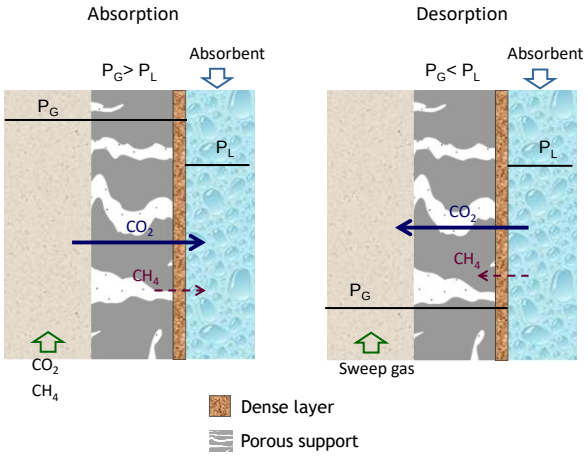

Figure 4: *Illustration of absorption and desorption using dense skin based membrane contactors*

This novel approach has the following advantages:

(i) Thanks to the dense membrane, water circulates in closed loop at a pressure set independently of biogas pressure. Thus, neither water depressurization before the desorber nor water recompression before the absorber is needed.

(ii) Thus, compared to the conventional process, the high pressure pump, the flash vessel and the heat exchanger are substituted by a simple pump, leading to a potential decrease of the energy requirement of the process (i.e. OPEX). A single cheap equipment (circulating pump) is needed, which generates lower capital expenses (i.e. CAPEX).

(iii) The selectivity of the dense skin typically of around 10 to above 60 (polyimide, cellulose acetate, perfluoropolymers) in favor of CO_2, could potentially decrease methane losses in the liquid phase during the absorption/desorption steps.

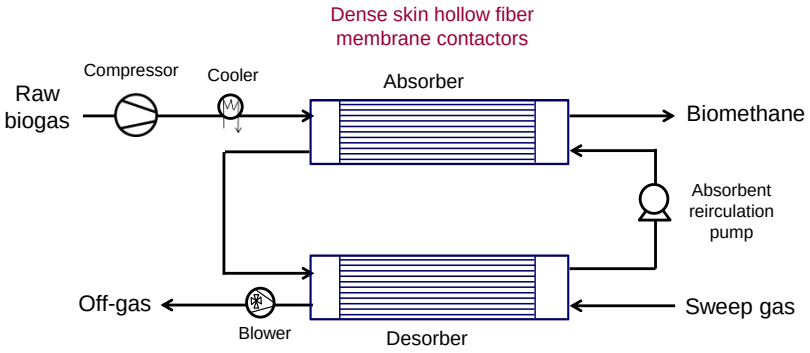

Figure 5: *Novel HFMC based absorption/desorption loop for biogas purification by pressurized water*

4. Dense membrane based HFMC for biogas purification by pressurized water : state of the art

Experimental studies based on non-porous membrane for CO_2 absorption using water as absorbent are summarized in **Table 2. Ozturk and Hughes (2012)** and **Heile et al., (2014)** used dense thick selfstanding silicone rubber HFMC, of 165 μm and 35μm membrane thickness respectively. **Belaissaoui et al., (2016)** used dense skin PolyPhenylene Oxide (PPO) based HFMC from Parker and **Kerber et al., 2016** tested a polydimethylsiloxane (PDMS) coated and a Teflon-AF coated composite flat-sheet gas permeation membrane (PolyActive™). In these studies, it was shown that liquid phase controls the mass transfer and that the dense layer membrane used can effectively prevent wetting. In addition, it was shown experimentally that similarly to PWA process in packed columns, there is a trade-off between biogas purity and process selectivity towards methane.
Regarding the mechanical resistance of dense membranes, **Trusov et al., 2011** showed experimentally that dense based glassy membrane (thickness of 20μm to 40μm) can operate successfully under transmembrane pressure difference of 40 bar when tested for CO_2 desorption from pressurized water. Based on theoretical calculation, it has been shown that a thickness as low as 5μm can support up to 10 bar transmembrane difference [**Chabanon *et al*., 2014**].

Polymeric membranes are widely used because of their ease of manufacture. The main commercially available membranes for CO_2 removal include cellulose acetate, polyimides and perfluoropolymers. The latter are highly resistant to plasticization. However, their performances are limited by the trade-off between permeability and selectivity described by the Robeson upper bound. Important efforts have been made to surpass this limitation as shown in **Figure B.1 in Appendix B**. High performing membranes include mixed matrix membrane (MMMs), facilated transport fixed site carrier membranes (FSCM), thermally rearranged polymers, and polymers with intrinsic micro-porosity (PIMS). **Table 3** gives an example of polymers performances.

Membrane type	T_L (°C)	Operating pressure conditions	Feed gas and flow arrangement	u_L (m/s)	u_G(m/s)	$k_{m,CO2}$ (m/s)	$k_{ov,CO2}$ (m/s)	$k_{ov,CO2}.a$ s^{-1}	Average CO_2 flux mol/m^2.s	Main observations/conclusions	References
Dense self-standing Silicone Rubber HFMC *Dow Corning Corporation* e = 165µm a= 500 m^{-1}	20	P_G/P_L=0.1 to 2.5 P_G= 0-25 bar	10% CO_2/N_2 in lumen side	Re_L= 60- 200	-	$1.5.10^{-5}$ m/s	6.10^{-6} (mean value)	3.10^{-3} (mean value)	2.10^{-5} to 4.10^{-5}	• CO_2 removal increases slightly with increasing liquid velocity • The fractional removal of CO_2 is also increased by increasing pressure ratio • Permeation rate of CO_2 increases 2.5 times when the pressure ratio was increased 2.5 times. • Selectivity[a] of CO_2/N_2 decreases by 50% when the pressure ratio was increased 2.5 times.	Ozturk and Hughes, 2012 Al- Saffar *et al.*, 1997
Asymmetric glassy flat-sheet membrane e =20-40 µm	100	P_G= 10 bar (P_L-P_G) =40 bar	Pure CO_2	0 to 0.1	-	$1.5.10^{-4}$ to $1.6.10^{-3}$ (at 25°C)	-	-	0.01-0.05	• **Desorption experiments** • No vacuum or stripping gas was used • No change in the chemical structure and macroscopic properties of those polymers, on long term tests.	Trusov *et al*., 2011
Dense self-standing polydimethylsiloxane (PDMS) HFMC *PermSelect*® e = 35µm a=4156 m^{-1}	19-22	-	20%, 40%, 80% CO_2 in CH_4 in the shell side	0 to $2.5.10^{-2}$	0 to 0.84	-	$2.4.10^{-6}$ to 5.10^{-6}	10^{-2} to 2.10^{-2}	0 to 4.10^{-4}	• CO_2 absorption flux increases with increasing liquid velocity • The outlet CO_2 content declines with increasing liquid velocity • Process selectivity [b] (CO_2/CH_4) decreases with increasing liquid velocity and attain a plateau • CO_2 absorbed flux increases with feed CO_2 content	Heile et al, 2014
Composite membranes of PPO (1µm dense skin layer +porous support) HFMC *Parker* e = 75µm a_{total}=1224m^{-1}	22	P_G/P_L=0.89 P_G=2.5 bar P_L=2.8 bar	30% CO_2/CH_4 in the lumen side	1.10^{-4} to 4.10^{-4}	u_L/u_G =0.04 - 0.13	5.10^{-4}	1.10^{-6} to 3.10^{-6}	$1.2.10^{-3}$ to $3.6.10^{-3}$	1.10^{-5} to 3.10^{-5}	• Methane loss decreases with increasing gas velocity and was below 4% • CO_2 removal efficiency varies from 10 to 80% • Liquid phase controls the mass transfer • CO_2 absorbed flux increases with increasing liquid velocity	Belaissaoui *et al.*, 2016
PDMS coated and a Teflon-AF coated composite flat-sheet membrane *(PolyActive™)* e_{total} = 162 µm a=667m^{-1} α_{PDMS} = 9.6 (dry pure gas measurement)	25	P_G/P_L=1 to 3 P_L=1-5 bar P_G=1-7 bar $(P_G-P_L)_{max}$ =2 bar	Various CO_2/CH_4 gas mixtures, in the lumen side	Q_L = 10-50 l/h	-	PDMS : 6.10^{-5} to 1.210^{-4} Teflon : $2.1.10^{-5}$ to 2.410^{-5}	PDMS : $1.6.10^{-5}$ to $2.1.10^{-5}$ Teflon : 1.10^{-5} to $1.3.10^{-5}$	PDMS : 1.10^{-2} to $1.4.10^{-2}$ Teflon : $6.7.10^{-3}$ to $8.7.10^{-3}$	0 to 6.10^{-3}	• Both membrane and solvent governed the transmembrane flux and the selectivity of the process • A high-pressure level greatly improved the transmembrane flux due to the increase of the driving force • PDMS shows a better performance compared to the Teflon-AF coated membrane • For pressure ratio above 2, process selectivity[a] increases with increasing pressure ratio	Kerber and Repke, 2016

[a]Process selectivity is defined as a ratio of K_{CO2}/K_{CH4} (K_{CO2} and K_{CH4} are CO_2 and CH_4 global masse transfer coefficients respectively).
[b]Process selectivity is defined as the separation factor of CO_2/CH_4 mixture.

Table 2: A synthesis of recent literature studies on CO_2 absorption using dense gas-liquid membrane contactors and water as absorbent. Desorption experiments are indicated.

Table 3: *Example of polymeric membranes for CO_2/CH_4 separation.*

	CO_2 permeability (barrer)	CO_2/CH_4 selectivity (-)	$K_{M,CO2}$ * (m/s)	T (°C)	P (bar)	Reference
Polyimide	0.63	98	$5.4.10^{-7}$	25	1	Scholes *et al.*, 2012
Cellulose acetate	6	29	5.10^{-6}	35	-	Scholes *et al.*, 2012
Matrimid 5218	9	41	7.10^{-6}	35	7.5	Chen *et al.*, 2011
Teflon AF2400	2200	5.7	2.10^{-3}	35	27	Merkel, 2006
PIM 1	2300	18.4	2.10^{-3}	30	-	Budd *et al.*, 2005
PPO (*Parker*) (Memb. A)	600	17	5.10^{-4}	-	-	Pourafshari *et al.*, 2006 Belaissaoui *et al.*, 2016
Polyimide (*Evonik*) (Memb. B)	60	60	5.10^{-5}	-	-	Scholz *et al.*, 2013
*calculated assuming a dense skin thickness of 1µm						

5. Simulation framework

5.1. 1D model – resistances in series model

The membrane module has been modelled according to 1D resistances in series approach, similarly to previous studies dedicated to gas liquid absorption processes [Z. Cui and D. DeMontigny, 2013, D. Albarracin Zaidiza et al., 2014]. A 1D modeling strategy systematically separately considers the three different mass transfer domains shown in **Figure 6** in order to determine the effective local mass transfer coefficient of specie *i*, $k_{ov,i}$. Absorption and desorption processes are assumed to be isothermal. In **Appendix C**, details on model assumptions, gas and liquid mass transfer coefficient calculation as well as differential equation system solved for counter current absorption/desorber membrane contactor simulation are presented. For all simulation, the liquid circulate in the shell side of the fiber while the gas flows in the lumen side.

The simulation methodology of the absorber/desorber process is sketched in **Figure 7**.

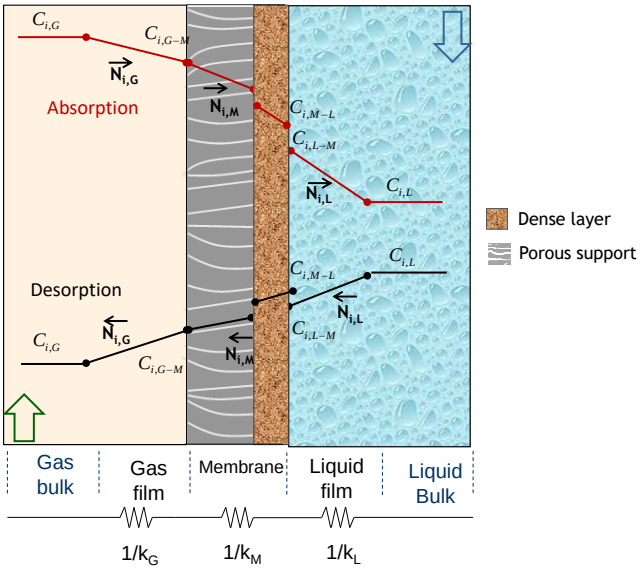

Figure 6: *A schematic representation of the resistances in series based on film theory*

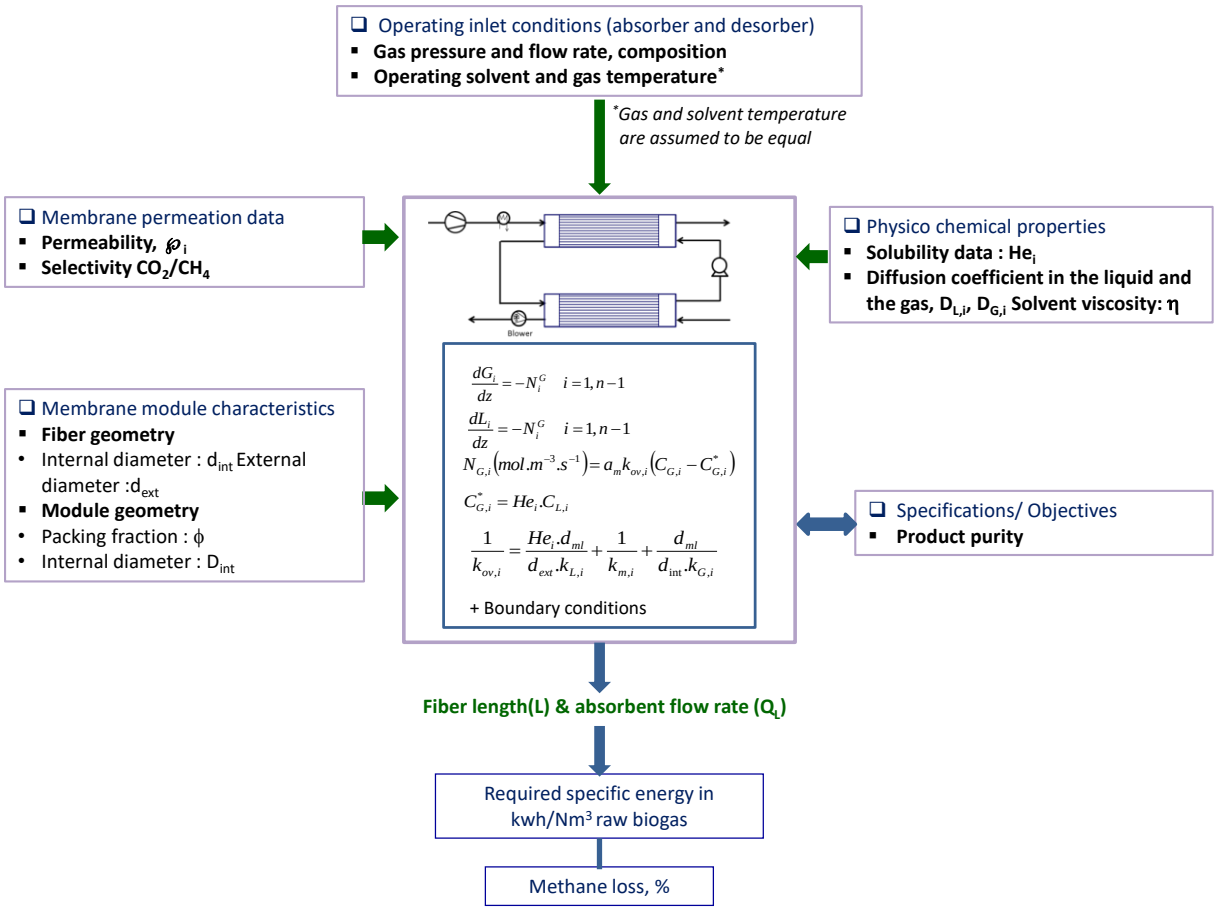

Figure 7 : *Scheme of the simulation methodology*

5.2. Membrane module characteristics and simulation conditions

Geometrical characteristics of the hollow fiber membrane module (HFMC) are illustrated in **Figure 8**. In the simulation, the fiber geometry of commercial PPO (Parker P-240) is considered. The packing fraction and the module internal diameter were set 0.5 and 36 cm respectively, which is typical of industrial modules. The characteristics of the membrane module are summarized in **Table 4**.

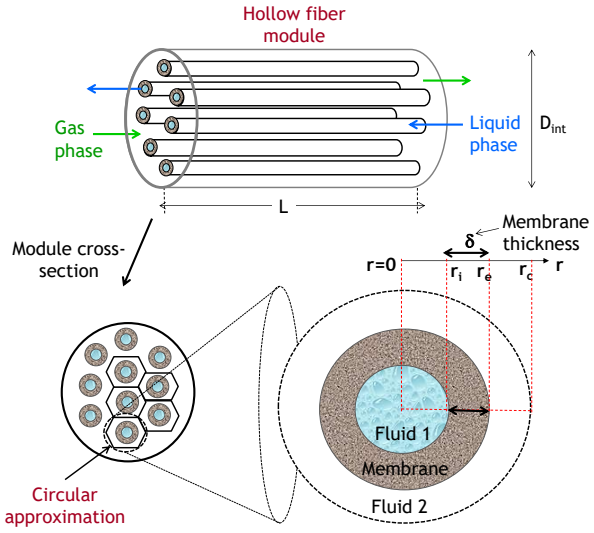

Figure 8: *Geometrical characteristics of the hollow fiber membrane module (HFMC)*

***Table 4**: Characteristics of the membrane module for all simulations.*

	Characteristics	Value
Module	Inner diameter (m), D_{int}	0.36
	Packing ratio (-), ϕ	0.50
	Fiber number (-), N	$2.39.10^5$
	Mean log specific interfacial area (m^{-1}), a	3260
Fiber	Inner diameter(μm), d_{int}	370
	Outer diameter(μm), d_{ext}	520

5.3. Simulation conditions

In the simulation, the gas is considered to be a binary CO_2/CH_4 mixture, composed of 35% CO_2 and 65% CH_4 (typical composition of raw biogas). Raw biogas is compressed to 8 bar [**Nock at al., 2014, Budzianowski, 2017]** according to typical relevant industrial conditions for biogas purification application. After compression, biogas is cooled at 15°C before entering the absorber where water available at 15°C flows counter-currently. In the gas leaving the absorber, 98% biomethane purity is aimed. CO_2 rich solvent leaving the absorber meets then a counter flow of nitrogen gas sweep at atmospheric pressure and 15°C circulating using a blower. Nitrogen is supposed to not transfer across the membrane. The regenerated water leaving the desorber is recycled back to the absorber in a closed loop (**Figure 5**). In the simulations, the solvent and the gas phase circulate through the shell and through the lumen of the fibers respectively.
The operating conditions considered in the simulations are summarized in **Table 5**. The physico-chemical properties and phase equilibria data of the system at 15°C are given in **Table 6**.

***Table 5** : Operating conditions of all simulations*

	Absorber	Desorber
Gas inlet composition	65% CH_4 35% CO_2	N_2
Temperature (°C)	15	15
Gas inlet flowrate (Nm^3/h)	55.55	119
Gas inlet pressure (bar)	8	1.12
Inlet gas interstitial velocity (m/s)	0.08	1.22

***Table 6** : Physico-chemical properties and phase equilibria data of the system at 15°C.*

	CO_2	CH_4
Henry's constant (-) $(C_G/C_L)eq$ [a]	0.92	24.73
Diffusion coefficient in liquid phase (m^2/s) [b,c]	$9.4.10^{-10}$	$9.7.10^{-10}$
Diffusion coefficient in gas phase (m^2/s) [d,e]	$1.2.10^{-5}$	$1.7.10^{-5}$
Absorbent solubility CO_2/CH_4 selectivity (-)	26.88	
Absorbent viscosity (10^{-3} Pa.s)	1.14	
[a] R. Sander, compilation of Henry's law, [b] Versteeg GF, Van Swaaij 1988, [c] Guo H, 2013, [d] Wylock 2014, [e] Cowie Watt., 1971.		

5.4. Process performance and energy requirement

The main performance indicators to be evaluated for gas-liquid HFMC for CO_2 removal from biogas purification are:

- Average overall CO_2 mass transfer coefficient $K_{ov,\,CO2}$ in m/s
- The product of $K_{ov,CO2}$×a in s^{-1}, with *a* the specific membrane area in m^{-1}.
- Average CO_2 absorbed volumetric flux in $mol/m^3.s$
- CO_2 removal efficiency, η_{CO2} (%)
- Process specific energy requirement in kWh/Nm^3 of raw biogas.

- CH_4 recovery or methane loss (%)

By writing a mass balance across a differential section of the membrane contactor, then integrating over the length of the contactor, the average CO_2 absorbed flux and overall CO_2 mass transfer coefficient K_{ov} is calculated. The possibility for membrane contactors to achieve process intensification compared to packed columns has been evaluated by comparing $k_{ov,\,CO2}.a$ values for both technologies.

CO_2 removal efficiency η_{CO2} is calculated as:

$$\eta_{CO2} = \frac{Q_{G,in} \times y_{CO2,in} - Q_{G,out} \times y_{CO2,out}}{Q_{G,in} \times y_{CO2,in}} \qquad (1)$$

Where $Q_{G,in}$ and $Q_{G,out}$ are the gas flow rates at the inlet and outlet of the membrane contactor, respectively. $y_{CO2,in}$ and $y_{CO2,\text{out}}$ are the CO_2 molar fraction at the gas inlet and outlet respectively.
Similarly, the loss of methane by absorption in the liquid can be calculated by:

$$Loss_{CH4} = \frac{Q_{G,in} \times y_{CH4,in} - Q_{G,out} \times y_{CH4,out}}{Q_{G,in} \times y_{CH4,in}} \qquad (2)$$

The power requirement of water scrubbing varies depending on plant configurations and operating conditions. The energy requirement for the HFMC based depicted in **Figure 5** is the summation of different contributions corresponding to:

- Raw biogas compression, $P_{BG,C}$
- Cooling of the compressed raw biogas up to the absober operating temperature, $P_{BG,cooling}$
- Water pumping power requirement for the recirculation of water in closed loop, $P_{L,p}$
- Blowing gas sweep to strip CO_2 from CO_2-loaded water, $P_{b,sweep}$

To estimate the power requirement of the compressor, isentropic compression was assumed.

$$P_{BG,C} = \frac{1}{\eta_C} G_{in,biogas} \frac{\gamma RT}{\gamma - 1} \left[\left(\frac{P_{G,abs}}{P_{in}} \right)^{\frac{\gamma-1}{\gamma}} - 1 \right] \qquad (3)$$

With T is the inlet temperature (in K) and R is the gas perfect constant (R= 8.314 J/(mol.K)). γ is the adiabatic expansion factor of the gas mixture. η_c is the compressor efficiency. $G_{in,biogas}$ is the molar flow rate of raw biogas.
Biogas temperature increases during compression thus biogas is cooled subsequently to reduce its temperature. Biogas compressor outlet temperature T_{G2} was calculated from biogas inlet temperature T_{G1} as follows:

$$T_{G2} = T_{G1} \frac{P_{G,abs}}{P_{in}}^{\frac{\gamma-1}{\gamma}} \qquad (4)$$

With P_{in}, the raw biogas pressure prior to compression and $P_{G,abs}$ is the biogas pressure at the inlet of the absorber.
Cooling using water is considered with water temperature variation of 10K **[Nock et al., 2014].** The flow rate of the coolant in the heat exchanger was calculated as follows:

$$Q_{Watercoolant} = \frac{Q_{biogas}.\rho_{biogas}.Cp_G(T_{G2} - T_{G1})}{\rho_L.Cp_L(T_{L1} - T_{L2})} \qquad (5)$$

The power requirement for cooling the biogas was then calculated from Equation 6 using the flow rate of the coolant with ΔP equal to the relative pressure of the gas inlet in the absorber. Q_{biogas} is the raw biogas flow rate at the compressor outlet. Cp_G and Cp_L the specific heat of the gas and the water coolant respectively.

The recirculation pump has to pressurize the lean solvent to the operating pressure of the absorption column. The required energy demand for water absorbent pumping is calcuted fom the solvent flow rate, Q_L, and total liquid pressure drop ΔP_L by :

$$P_{L,p} = \frac{1}{\eta_p} Q_L . \Delta P_L \quad (6)$$

η_p is the pump efficiency. The pressure drop in the lumen and shell side is calculated using Hagen Poiseuille and Happel equations respectively.

The power requirement for blowing air, $P_{b,sweep}$ is calculated from gas sweep flow rate, Q_{sweep} and sweep gas pressure drop in the desorber, ΔP_{sweep} ,as following :

$$P_{b,sweep} = \frac{1}{\eta_B} Q_{sweep} . \Delta P_{sweep} \quad (7)$$

η_b is the blower efficiency.

Table 7 summarizes the assumptions made in power requirements calculation.

Table 7: *Assumptions made in power requirements calculation.*

Variable	value
Pump efficiency, η_P	0.6
Blower efficiency, η_B	0.6
Compressor efficiency, η_C	0.8
Adiabatic expansion coefficient, γ	1.3

The specific energy requirement in kwh/Nm^3 of raw biogas is calculated by dividing the power requirement by the inlet raw biogas flow rate in Nm^3/h.

6. Results and discussion

Figure 9 shows the simulation results using membrane A (**Table 3**) for both absorber and desorber. Streams flow rate and concentrations are also indicated. **Figures 10a** and **10b** show the axial profile of CO_2 and CH_4 transmembrane flux in the absorber and desorber respectively. At the gas inlet, CH_4 flux is almost zero indicating that the outlet liquid is near 100% saturation in CH_4. In fact the liquid was saturated at 95% in methane and only at 40% in CO_2. CH_4 flux increases from the gas inlet as the driving force between the two phases increases. An inverse profile is observed for CO_2. CO_2 flux is minimal at the gas outlet where the CO_2 content is constrained to 2% and where the driving force between the two phases is minimal. The flux increases from the gas outlet as the driving force between the two phases increases. In the desorber CO_2 and CH_4 flux follow the same trend. Fluxes are maximal at the liquid inlet (CO_2 and CH_4 loaded solvent) and decreases as the gaseous species are desorbed from the liquid phase.

Using commercially available dense based HFMC, the process is able to recover 96.6 % of CO_2 and reach biomethane purity of 98%. The energy requirement, overall mass transfer coefficient and gas recovery are shown in **Table 9**. The corresponding energy requirement is of 0.17 kWh/Nm^3 raw biogas, which is 20 to 35% lower than that reported for packed column based process, under comparable gas inlet conditions and separation specifications as can be seen in **Tables 10 and Table D.1** in Appendix A**.** However, the obtained methane loss is around 8% which is significantly higher than that reported for conventional packed column based process (less than 2%). In the latter, flash thank is used to recover methane from rich absorbent. The recovered methane is then recycled to the inlet of the absorber (**Figure2**).

The $k_{ov,\,CO2}.a$ values obtained in this work, given in **Table 9** (0.025-0.05 s^{-1}), are near the upper bound of baseline technology (packed column) ranging from 6×10^{-4} to 7×10^{-2} s^{-1}[Elhajj et al., 2014].

However, values reported for packed column under comparable feed conditions and product specification are scarce. Value of $k_{ov,\,CO2}.a$ in literature corresponding to papers referenced in **Table 10** are not systematically provided at the exception of the work of **Nock et al., 2014.** They reported a (K_{ov}.a) value of 0.028 s^{-1} for the absortion column. Taken this value as a reference, the proposed process shows intensification factor of about 1.68, corresponding to a volumetric reduction of about 68%.

Given that liquid side mass transfer coefficient is about one and two orders of magnitude lower than that of the membrane in the absorber and desorber respectively, process selectivity is controlled by the selectivity of the absorbent. Thus, it can be anticipated that no significant methane loss reduction will be obtained from increasing membrane selectivity as soon as process selectivity is controlled by the absorbent. In order to evaluate, under the same operating conditions, the interest of higher membrane selectivity for methane loss reduction, the process is simulated using Membrane B (**Table 3**), having a CO_2/CH_4 selectivity of 60, for both absorber and desorber. The corresponding absorber and desorber length has been determined to fulfill the target of 2% CO_2 content in biogas product.
The results are shown in **Figure 11**.
Increasing membrane selectivity from 17 (Membrane A) to 60 (Membrane B) with CO_2 membrane mass transfer coefficient ($k_{M,CO2}$) of 5.10^{-4} and 5.10^{-5} m/s respectively, leads to a very slight CH_4 loss reduction from 8.7% to 7.8% (10% reduction).

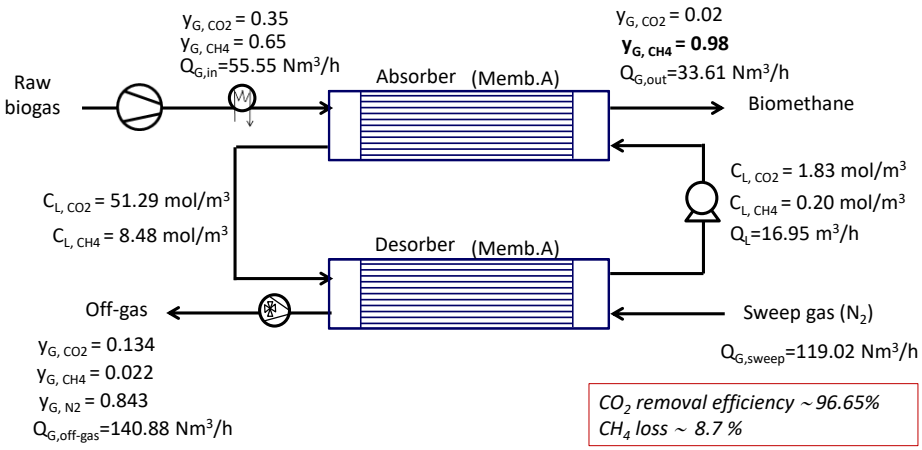

Figure 9: *Simulation results of the HFMC process for CO_2 removal from biogas using pressurized water. Partial regeneration of the absorbent. Simulation using membrane A (**Table 5**) for both absorber and desorber ($K_{m,CO2}$=5.10^{-4} m/s , CO_2/CH_4 selectivity of 17).*

(a) Absorber (b) Desorber

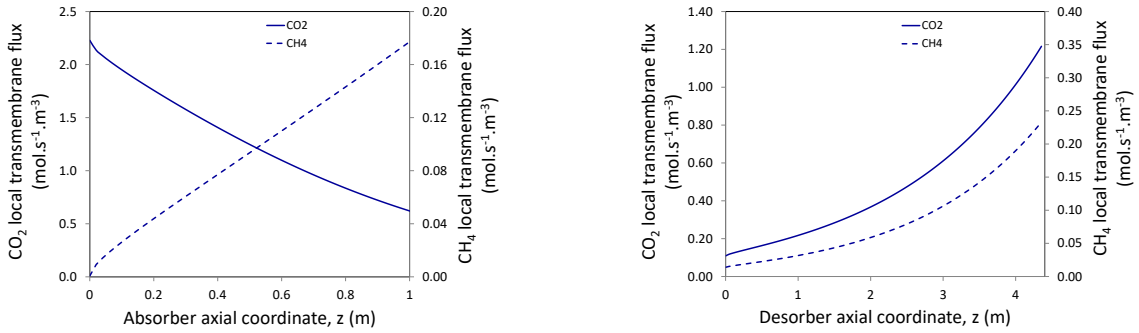

Figure 10: *CO_2 and CH_4 transmembrane flux profiles along the absorber. Configuration1. (a) absorber (b) desorber. z=0 corresponds to the gas inlet.*

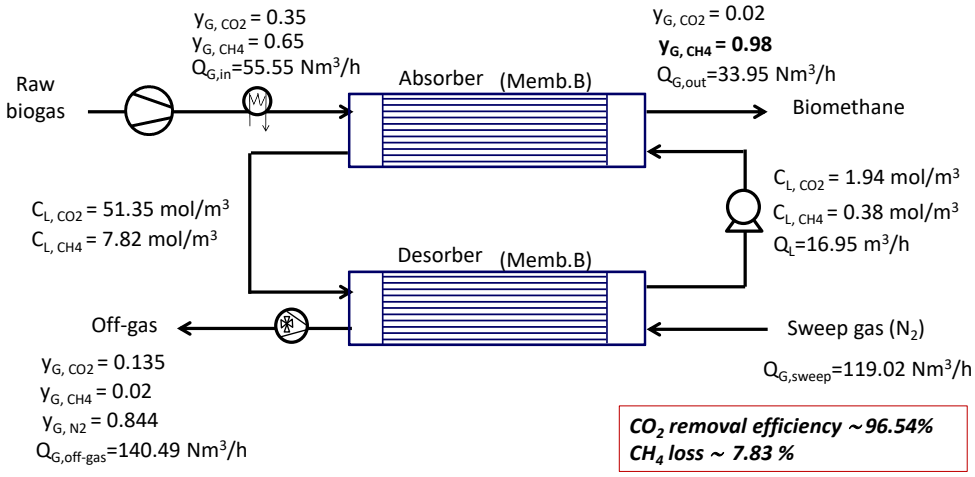

Figure 11: *Simulation results of the HFMC process for CO_2 removal from biogas using pressurized water. Partial regeneration of the absorbent. Simulation using membrane B (**Table 5**) for both absorber and desorber ($K_{m,CO2}$=5.10^{-5} m/s , CO_2/CH_4 selectivity of 60).*

Table 9*: Simulation results*

	Membrane A	Membrane B
Total liquid pressure drop (bar)	2.43	2.89
Absorber length (m)	2	2.5
Desorber length (m)	6	7
Liquid flowrate (m^3/h)	16.95	16.95
Liquid interstitial velocity (m/s)	0.09	0.09
Liquid recirculation (pumping) (kWh/Nm^3)	0.035	0.04
Biogas compression and cooling (kWh/Nm^3)	0.116	0.116
Sweep gas blower (kWh/Nm^3)	0.020	0.024
Total specific energy requirement (kWh/Nm^3)	0.170	0.182
$k_{ov,CO2}$ ($m.s^{-1}$) abs/des	$1.45.10^{-5}$ /$9.54.10^{-6}$	$1.15.10^{-5}$ /8.10^{-6}
$k_{ov,CO2}$. a (s^{-1}) abs/des	0.047/0.031	0.037/0.026
Average CO_2 specific absorbed flux (mol/m^3.s)	1.14	0.914
Average CO_2 specific stripped flux (mol/m^3.s)	0.38	0.33
CO_2 recovery ratio (%)	96.65	96.54
CH_4 purity (%)	98	98
CH_4 loss (%)	8.7	7.8

***Table 10**: Comparison with literature data*

Reference	Operating conditions[a] in the absorber	Methane purity (%)	Methane loss (%)	Raw biogas compression and cooling requirement (kWh/Nm^3raw biogas)	Absorbent pumping requirement (kWh/Nm^3raw biogas)	Total energy[b] requirement (kWh/Nm^3raw biogas)
This work (Memb.A)	Binary CH_4 65%/CO_2 P_G= 8bar 15°C	98 (2% CO_2)	8.7	0.116	0.034	0.17
Budzianowsky et al., 2017	Binary CH_4 65%/CO_2 P_G= 8bar 15°C	98	0.21	0.12	0.08	0.21
Nock et al., 2014	Binary CH_4 65%/CO_2 P_G= 10bar	98	<1	0.13	0.09	0.25-0.26
Xu et al., 2015	Binary CH_4 60%/CO_2 P_G= 8.2bar	98	1.3	-	-	0.212

[a] stripping pressure is around atmospheric pressure
[b] without further compression of the biomethane product

7. Conclusions and perspectives

This study aimed to evaluate the potentialities of a novel absorption/desorption loop using dense based HFMC technology for biogas purification using water as absorbent. . Through simulations, the following conclusions have been obtained:

(i) Using commercially available dense based HFMC, the process is able to recover 96.6 % of CO_2 and reach biomethane purity of 98%. The corresponding energy requirement is of 0.17 kWh/Nm^3 raw biogas, which is 20 to 35% lower than that reported for packed column based process, under comparable gas inlet conditions and product specifications.

(ii) Methane loss in the investigated operating conditions is around 8 % which is significantly higher than that reported for conventional packed column based process (less than 2%).

(iii) Considering the value of ($K_{ov,CO2}$.a) reported by Nock et al., (2014) for the absorber under comparable feed conditions and product specification, the novel HFMC process offers intensification factor of about 1.68, corresponding to a volumetric reduction of about 68% of the absorption unit.

(iv) Under the investigated operating conditions, liquid side mass transfer coefficient is about one to two orders of magnitude lower than that of the membrane in absorber and desorber respectively. Thus, process selectivity is mainly controlled by the absorbent. No significant process selectivity improvement is obtained from increasing membrane selectivity from 17 to 60 with $k_{M,CO2}$ of 5.10^{-4} and 5.10^{-5} m/s respectively.

A systematic and detailed parametric analysis (liquid and gas velocity, temperature, pressure, material permeation properties and module geometry) is needed in order to examine the interest of dense HFMC covering a wide range of operating conditions. Novel fiber geometries such as helices, waves or the addition of baffles could also be investigated in order to enhance the local turbulence in the liquid phase and thus mass transfer performances. These issues will be investigated in forthcoming papers.

More generally, the first simulation results of the proposed process raise several questions and the following perspectives can be proposed:

(i) In order to limit CH_4 loss, one flash should be added at medium pressure (between 8 to 5 bar) to recover a portion of CH_4 before entering the desorber contactor. The stripped CH_4 will be then compressed and recycled to the biomethane product. In this case recompression is still needed but is expected to be lower than in the conventional process where the flash is operated at near atmospheric pressure.

(ii) In order to recover CO_2 with high purity in the regeneration step, a sweep gas can be replaced by vacuum pumping in order to avoid dilution effect of N_2. In this case the required energy for vacuum pumping has to be evaluated.

(iii) The removal of trace compounds (N_2, O_2, H_2S, NH_3…) has not been investigated. The potential interest of dense skin selectivity towards these species is another potential advantage of dense skin contactors that would be interesting to investigate.

NOMENCLATURE

Latin symbols

a : Specific gas-liquid interfacial area (m^{-1})
d_h : Hydraulic diameter (m)
d_{int} : Internal fiber diameter (m)
d_{ext} : External fiber diameter (m)
d_{ml} : Log mean fiber diameter (m)
D_{int} : Internal membrane module diameter (m)
D_i : Diffusion coefficient ($m^{-2}\cdot s^{-1}$)
k : Mass transfer coefficient ($m\cdot s^{-1}$)
N_i : Molar flux (mol m^{-2} s^{-1})
P : Pressure (Pa)
Q : Fluid volumetric flow rate ($m^3.s^{-1}$)
ΔP : Fluid pressure drop (bar)
G : Gas molar flow rate ($mol.s^{-1}$)
L : Liquid molar follow rate ($mol.s^{-1}$)
Cp_G : Specific heat of the gas (J/kg.K)
Cp_L : Specific heat of the liquid (J/kg.K)
T_{G2} : Raw biogas temperature at the compressor outlet (K)
T_{G1} Raw biogas temperature at the compressor inlet (K)
R : Perfect gas constant (R= 8.314 J/(mol.K)).
Sh : Sherwood number (-)
Gz : Graetz number (-)
Re : Reynolds number (-)
T : Temperature (K)
C : Molar concentration ($mole.m^{-3}$)
C_G^* : Hypothetical local gas-phase concentration in equilibrium with the liquid phase ($mol.m^{-3}$)
y : Molar fraction in the gas (-)
u : Interstitial fluid velocity ($m\cdot s^{-1}$)
He : Henry constant (C_G/C_L) (-)
z : Axial coordinate (m)
k_{ov} : overall mass transfer coefficient ($m.s^1$)
$P_{BG,C}$: Power required for raw biogas compression (W)
$P_{BG,cooling}$:Cooling of the compressed raw biogas up to the absober operating temperature (W)
$P_{L,p}$: Water pumping power requirement for the recirculation of water in closed loop(W)
$P_{b,sweep}$: Power required for blowing gas sweep to strip CO_2 from CO_2-loaded water(W)
η_c : Compressor efficiency (-)
$G_{in,biogas}$: Molar flow rate of raw biogas ($mol.s^{-1}$)
P_{in} : Raw biogas pressure prior to compression (bar)
$P_{G,abs}$: Raw biogas pressure at the inlet of the absorber (bar)
Q_{biogas} :Raw biogas flow rate at the compressor outlet ($m^3.s^{-1}$)
Q_{sweep} : Gas sweep flow rate ($m^3.s^{-1}$)
ΔP_{sweep} :Sweep gas pressure drop in the desorber (bar)

Greek symbols

φ : Module packing ratio (-)
μ : Viscosity ($Pa\cdot s^{-1}$)
ρ : Density ($kg\cdot m^{-3}$)
η_{CO2} : CO_2 removal efficiency (-)
Ω : Contactor cross section (m^2)
γ : Adiabatic expansion factor of the gas mixture (-)
η_c : Compressor efficiency (-)
η_B : Blower efficiency (-)

η_P : Pump efficiency (-)

Subscripts/ Exponents

i : Compound
G : Relative to gas
L : Relative to liquid
m : Relative to the membrane
in : Relative to fluid inlet
out : Relative to fluid outlet

References

References

Raven R.P.J.M., Gregersen, K.H. Biogas plants in Denmark: successes and setbacks, Renewable and Sustainable Energy Reviews, Volume 11, Issue 1, January 2007, Pages 116-132.

Annual Report of the International EnergyAgency2013.
https://www.iea.org/publications/freepublications/publication/2013_AnnualReport.pdf

M. Persson, Evaluation of upgrading techniques for biogas, Report SGC 142 ISSN 1102-7371 ISRN SGC-R--142—SE, Lund Institute of Technology, ©Swedish Gas Center - November 2003.

Gabelman A., Hwang, S-T, Hollow fiber membrane contactors, Journal of Membrane Science, Volume 159, Issues 1–2, 1 July 1999, Pages 61-106.

E. Drioli, E. Curcio, G. di Profio, State of the Art and Recent Progresses in Membrane Contactors, Chemical Engineering Research and Design, Volume 83, Issue 3, March 2005, Pages 223-233.

Belaissaoui B., Claveria-Baro J., Lorenzo-Hernando A. et al., Potentialities of a dense skin hollow fiber membrane contactor for biogas purification by pressurized water absorption, Journal of Membrane Science, Volume 513, 1 September 2016, Pages 236-249.

Ozturk B., Hughes R., Evaluation of mass transfer characteristics of non-porous and microporous membrane contactors for the removal of CO_2, Chemical Engineering Journal 195–196 (2012) 122-131.

Heile. S, Rosenberger S., Parker A., Jefferson B., McAdamE.J. Establishing the suitability of symmetric ultrathin wall polydimethylsiloxane hollow-fibre membrane contactors for enhanced CO_2 separation during biogas upgrading, Journal of Membrane Science 452 (2014) 37-45.

Kerber J., Repke, J-U, Mass transfer and selectivity analysis of a dense membrane contactor for upgrading biogas, Journal of Membrane Science, Volume 520, 15 December 2016, Pages 450-464.

Bauer F., Hulteberg C., Persson T., Tamm D., Biogas upgrading – Review of commercial technologies, SGC Rapport 2013:270.

Nock W. J., Walker M., Kapoor R., and Heaven S., Modeling the Water Scrubbing Process and Energy Requirements, for CO2 Capture to Upgrade Biogas to Biomethane, Ind. Eng. Chem. Res. 2014, 53, 12783−12792.

Garnaud D. and Zick G., application des membranes pour l'épuration du biogaz, Récents progrès en génie des procédés, numéro 105-2014.

Petersson, A., WELLINGER A. Biogas upgrading technologies –developments and innovations, IEA BIOENERGY report, 2009.IE
https://www.infothek-biomasse.ch/images/175_2009_IEA_Biogas_upgrading_technologies.pdf

Scholz M. Melin T., Wessling M.Transforming biogas into biomethane using membrane technology, Renewable and Sustainable Energy Reviews 17(2013)199–212.

Hoyer K., Hulteberg C., Svensson M., Jernberg Josefina and Nørregård Øyvind, Biogas upgrading - Technical Review, REPORT 2016:275.
http://vav.griffel.net/filer/C_Energiforsk2016-275.pdf

Budzianowski Wojciech M., Wylock Christophe E., Marciniak Przemysław A., Power requirements of biogas upgrading by water scrubbing and biomethane compression: Comparative analysis of various plant configurations, Energy Conversion and Management, Volume 141, 1 June 2017, Pages 2-19.

Trusov A., Legkov S., Van den Broeke L. J.P., Goetheer E., Volkov A., Gas/liquid membrane contactors based on disubstituted polyacetylene for CO_2 absorption liquid regeneration at high pressure and temperature. Journal of Membrane Science, Volume 383, Issues 1–2, 1 November 2011, Pages 241-249.

Chabanon E., Belaissaoui B., Favre E., Gas–liquid separation processes based on physical solvents: opportunities for membranes, Journal of Membrane Science, Volume 459, 1 June 2014, Pages 52-61.

Al-saffar H.B., Ozturk B., Hughes R., A Comparison of Porous and Non-Porous Gas-Liquid Membrane Contactors for Gas Separation, Chemical Engineering Research and Design, Volume 75, Issue 7, October 1997, Pages 685-692.

Scholes C. A., Stevens G.W., Kentish S. E., Membrane gas separation applications in natural gas processing, Fuel 96 (2012) 15–28.

Chen GQ, Scholes CA, Qiao GG, Kentish SE. Water vapor permeation in polyimide membranes. J Membr Sci 2011;379:479–87.

Merkel TC, Pinnau I, Prabhakar R, Freeman B. Gas and transport properties of perfluoropolymers. In: Yampolskii Y, Pinnau I, Freeman B, editors. Materials, science of membranes for gas and vapor separation. Chichester: John Wiley & Sons; 2006.

Budd P.M., Msayib KJ., Tattershall. CE. *et al*. Gas separation membranes from polymers of intrinsic microporosity, JOURNAL OF MEMBRANE SCIENCE Volume: 251 Issue: 1-2 Pages: 263-269 Published: APR 1 2005.

Pourafshari Chenara M., Soltanieha M., Matsuurab T., Tabe-Mohammadib A., 1, C. Feng, Gas permeation properties of commercial polyphenylene oxide and Cardo-type polyimide hollow fiber membranes, Separation and Purification Technology 51 (3) (2006) 359–366.

Sander R. (1999) Compilation of Henry's Law Constants for Inorganic and Organic Species of Potential Importance in Environmental Chemistry.
http://www.mpch-mainz.mpg.de/~sander/res/henry.html

Versteeg GF, Van Swaaij WPM. Solubility and diffusivity of acid gases (CO_2, N_2O) in aqueous alkanolamine solutions. J Chem Eng Data 1988;33:29–34.

Guo H, Chen Y, Lu W, Li L, Wang M. In situ Raman spectroscopic study of diffusion coefficients of methane in liquid water under high pressure and wide temperatures. Fluid Phase Equilibria 2013;360:274–8.

Wylock C, Antuñano N, Arias PL, Haut B. Analysis of the simultaneous gas– liquid CO_2 absorption and liquid-gas NH_3 desorption in a hydrometallurgical Waelz oxides purification process. Int J Chem Reactor Eng 2014;12:1–14.

Cowie Watt. Diffusion of methane and chloromethanes in air. Can J Chem 1971;49:74.
Yajing Xu, Ying Huang, BinWu, Xiangping Zhang , Suojiang Zhang, Biogas upgrading technologies: Energetic analysis and environmental, Chinese Journal of Chemical Engineering 23 (2015) 247–254.
Yang L., Ge X., Wan C., Yu F., Li Y., Progress and perspectives in converting biogas to transportation fuels, Renewable and Sustainable Energy Reviews, Volume 40, December 2014, Pages 1133-1152.

Ryckebosch E., Drouillon, M. Vervaeren H., Techniques for transformation of biogas to biomethane, Biomass and Bioenergy, Volume 35, Issue 5, May 2011, Pages 1633-1645.

Baker, R.Future directions of membrane gas-separation technology, Membrane Technology, Volume 2001, Issue 138, October 2001, Pages 5-10.

Robeson L. M., The upper bound revisited, Journal of Membrane Science 320 (1–2) (2008)390-400.
Yuan Zhanga, Jaka Sunarso, Shaomin Liu, Rong Wang, Current status and development of membranes for CO_2/CH_4 separation: A review, International Journal of Greenhouse Gas Control 12 (2013) 84–107.

Rezakazemi M., Amooghin A. E., Montazer-Rahmati M. M., Fauzi I. A., Matsuura T., State-of-the-art membrane based CO_2 separation using mixed matrix membranes (MMMs): An overview on current status and future directions, Progress in Polymer Science, Volume 39, Issue 5, May 2014, Pages 817-861.

Beek W.J., Muttzall K.M.K., Heuven J.W., Transport Phenomena, Wiley (1999).

Skelland A.H. P., Diffusional Mass Transfer, R.E. Krieger Pub. Co. (1985).

Lévêque A., Les Lois de la transmission de chaleur par convection, Dunod, Paris, France (1928).

APPENDICES

Appendix A

Table A.1: Typical biogas composition and purification requirements [Yang et al, 2014, Scholes et al, 2013, E. Ryckebosch et al, 2011, Baker 2001, Persson, SW report 2003, Garnaud and Zick, 2014]

Component	Composition unit	Raw biogas		Purification requirements	
		Anaerobic digestion	Landfill biogas	Heat and electricity requirement	Pipeline injection and transportation
CH_4	%	45-75%	30-65	96-98	>0.96
CO_2	%	30-55	15-50	<2-4	<2-4
H_2O	%	3	-	32 mg/Nm^3	<0.01 (US)
H_2S	ppm	0-2000	30-500	<16	<4
O_2	%	0-5	0-3	<1	<0.5-3
H_2	%	-	0-3	-	-
N_2	%	0.01-6	<1-17	<1	-
NH_3	ppm	<100	0-5	-	<3mg/Nm^3
Typical biogas flowrate		100-2000Nm^3/h	500-20000Nm^3/h		
Typical inlet temperature		25-55°C and water saturated			
Pressure (bar)					2-9

Appendix B

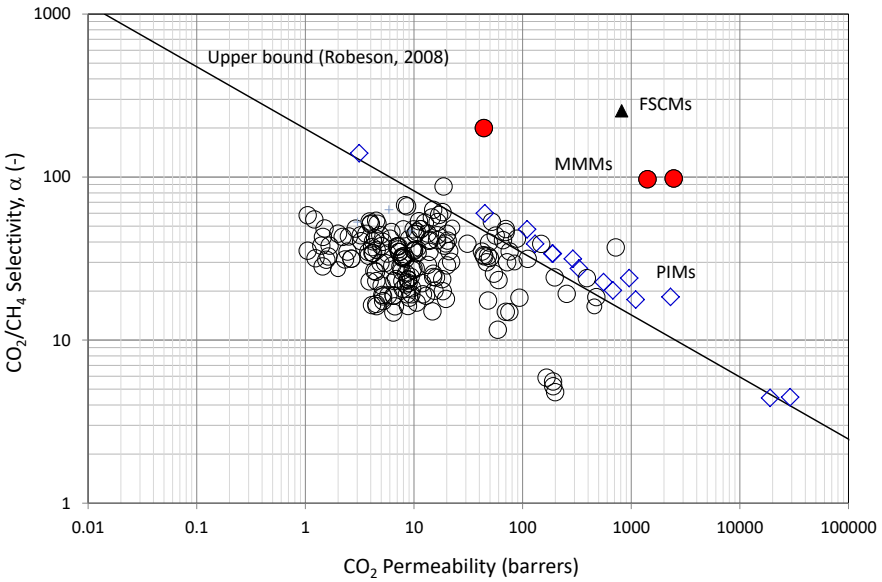

Figure B.1 *Permeability /selectivity trade-off and upper bound for CO_2/CH_4 separation [**Robeson, 2008**] – Data of polymeric and advanced FSCM, MMMs, PIMs are added [**Zhang et al, 2013, Mashallah et al, 2014, Scholes et al., 2012**].*

Appendix C : 1D model – resistances in series model

A resistances in series expression based on film theory is classically used in that case [Gabelman and Hwang, 1999]. The local overall mass transfer coefficients can be expressed according to the resistance- in series model as follows:

The local absorbed CO_2 molar flux of specie *i* is expressed as:

$$N_{G,i}\left(mol.m^{-3}.s^{-1}\right) = a_m k_{ov,i}\left(C_{G,i} - C^*_{G,i}\right) \qquad \text{(C1)}$$

Where:

$$\frac{1}{k_{ov,i}} = \frac{He_i.d_{ml}}{d_e.k_{L,i}}. + \frac{1}{k_{m,i}} + \frac{d_{ml}}{d_i.k_{G,i}} \qquad \text{(C2)}$$

$$C^*_{G,i} = He_i.C_{L,i} \qquad \text{(C3)}$$

a is the specific membrane module interfacial area (m^{-1}).
$C_{G,i}^*$ is the hypothetical local gas-phase concentration in equilibrium with the liquid phase.
$k_{ov,i}$ is the local global mass transfer coefficient of specie $_i$. $k_{L,i}$, $k_{M,i}$, $k_{G,i}$ are the local effective membrane mass transfer coefficients of the membrane, the liquid and the gas phase respectively.
d_{int}, d_{ext} d_{ml} are the inner, outer and log mean diameters of the hollow fiber membrane. *He* is the Henry constant of the gas compound with water (defined as : $He = C_G\ (mol/m^3)/C_L\ (mol/m^3)$) .

In this model, the film theory (diffusion in boundary layer) is applied in the liquid and gas phases. The key assumptions of the 1D model are:

- Constant membrane mass transfer ($k_{m,i}$) coefficient
- Plug flow for both gas and liquid phases
- Thermodynamic equilibrium at the gas–liquid interface

In laminar flow through a cylindrical pipe, gas and liquid mass transfer coefficient, k_G and k_L respectively can be estimated by integrating the Graetz equation [**Beek 1999, Skelland 1985, Levêque 1928**] for suitable boundary conditions.
The Sherwood number in each phase is estimated by:

if $Gz < 0.03$ then $Sh = 1.3Gz^{-1/3}$ (C4)
if $Gz > 0.03$ then $Sh = 4.36$ (C5)
With Graetz and Sherwood numbers defined as follows (z is the axial coordinate):

$$Gz = \frac{D.z}{u_G.d_h^{\,2}} \qquad \text{(C6)}$$

$$Sh = \frac{k d_h}{D} \qquad \text{(C7)}$$

With d_h the hydraulic diameter.

For the gas phase, flowing in the lumen side, d_h corresponds to the internal fiber diameter (d_i).

The 1D model takes into account the evolution of the local mass transfer coefficients, the evolution of gas velocity (due to CO_2 absorption) and fluid pressure through the axial coordinate (z).
The differential equation system which is solved is detailed hereafter (n is the components number):

- Gas differential molar balance:

$$\frac{dG_i}{dz} = -N_{G,i} \quad i = 1, n-1 \qquad \text{(C8)}$$

- Liquid differential molar balance:

$$\frac{dL_i}{dz} = -N_{G,i} \quad i = 1, n-1$$

(C9)

With

$$L_i = u_L C_{i,L} \quad \text{(C10)}$$

$$G_i = u_G C_{i,G} \quad \text{(C11)}$$

The boundary conditions are:

$$G_{G,i,z=0} = G_{z=0} \times y_{i,z=0}, \quad i = 1, n-1 \quad \text{(C14)}$$

$$C_{L,i,z=Z} = C_{L,i,0} \quad i = 1, n-1 \quad \text{(C15)}$$

$$C_{L,i,z=0} = C_{L,i,z=0}(initialisation) \quad i = 1, n-1 \quad \text{(C16)}$$

G_i, L_i, are the molar flow rate of compound *i* in the gas phase and in the liquid phase respectively. Equations (C8-C9) are numerically solved with the appropriate boundary conditions through a Matlab computer code.

Appendix D

Table D.1 *Detailed energy requirement comparison with values from literature.*

Energy requirement (kWh_{el}/Nm^3 raw biogas)	This work (Memb.A)	Budzianowsky et al., 2017	Nock et al., 2014
Raw biogas compression and cooling	0.116	~0.12	~0.13
Liquid pumping	0.034	~0.08	~0.09
Air blower	0.02	-	~0.01
TOTAL	0.17	0.21	0.25-0.26